Institut für Festkörperphysik (a) and Institut für angewandte Physik (b), Technische Hochschule Darmstadt[1])

Dielectric Investigation of α-$LiIO_3$

By

L. G. JACOBSOHN[2]) (a), P. LUNKENHEIMER[3]) (a), F. LAERI (b), U. VIETZE (b), and A. LOIDL[3]) (a)

The dielectric properties of hexagonal lithium iodate (α-$LiIO_3$) single crystals have been studied at frequencies 10^{-2} Hz $\leq \nu \leq 10^9$ Hz and temperatures 100 K $\leq T \leq$ 500 K. Pure and iron doped crystals were investigated. Below approximately 10 kHz, the electric response of the $LiIO_3$ crystals is almost entirely dominated by the accumulation of space charges at the electrodes. At least two types of ionic charge carriers seem to contribute to the observed conductivity. In addition, dc measurements revealed that electronic conductivity cannot be neglected in α-$LiIO_3$. At frequencies above some 100 kHz the real part of the conductivity σ' follows a power law $\sigma' \sim \nu^s$ with relatively small exponents s for both, the doped and the undoped compounds. The temperature dependence of σ' in this region behaves thermally activated with two energy barriers. The high-frequency limit of the dielectric constant ε_∞ has been determined. In addition, the data have been evaluated using the modulus formalism.

1. Introduction

The alpha modification of lithium iodate (α-$LiIO_3$) has attracted considerable attention in the past years due to its piezoelectric [1, 2], acousto-optic [2], and nonlinear optical properties [3, 4], which make this material well suited for ultrasonic applications, for laser technologies, and optoelectronic devices. At room temperature $LiIO_3$ reveals a hexagonal closed packed structure (α-phase) with Li^+ and I^{5+} ions occupying oxygen octahedral interstices [5]. It undergoes two phase transitions, into an orthorhombic structure (γ-phase) and into a tetragonal structure (β-phase) [6]. Even at room temperature, α-$LiIO_3$ exhibits a considerable and strongly anisotropic ionic conductivity. It is several orders of magnitude higher along the c-axis than along the a-axis [1, 7, 8]. The conductivity is mainly due to lithium ions, at least along the c-axis [9 to 12]. In this work, the dielectric properties were studied for hexagonal lithium iodate along the c-axis.

It is known that $LiIO_3$ is sensitive to the growing conditions, namely the temperature and the pH value of the original solution. These conditions affect the electrical [13], optical [14 to 16], and structural properties [6, 17]. The pH value is closely related to the presence of hydrogen impurities in the lattice [14]: iodic acid (HIO_3) and inclusions of H_2O have been detected. In optical absorption studies these impurities

[1]) Hochschulstr. 6, D-64289 Darmstadt, Germany.

[2]) Permanent address: Pontificia Universidade Católica do Rio de Janeiro, Departamento de Ciência dos Materiais e Metalurgia, 22453-900 Rio de Janeiro, R.J., Brazil.

[3]) Present address: Universität Augsburg, Experimentalphysik V, Universitätsstr. 2, D-86135 Augsburg, Germany.

can be identified [14 to 16, 18 to 21]. From these investigations, it is clear that HIO_3 is only present for growth conditions with solutions of pH ≤ 5, and H_2O seems to be present for pH values ≥ 5 to 6 only.

The best way to describe the presence of hydrogen in the lattice is by means of a non-stoichiometric compound of the type $Li_{1-x}H_xIO_3$ [22]. Hamid and coworkers [22, 23] studied the dielectric behaviour of this compound for different values of x in the range of 5 to 500 kHz, and identified a high dependence of the dielectric constant and the resistivity on the hydrogen concentration x. There are various reports on the conductivity and dielectric properties of α-$LiIO_3$ using dc and ac techniques covering a frequency range from 0.05 Hz to 1 GHz [1, 2, 7 to 9, 13, 19, 22 to 31]. However, it is difficult to get a conclusive picture of the electrical properties of α-$LiIO_3$ from these reports which have been obtained on crystals grown under different conditions and using different electrode materials. In addition, the presentation and interpretation of the data are often incomplete or even misleading, the main difficulty being the neglect of the influence of space charge effects in this ionic conductor. Therefore, we performed dielectric measurements of α-$LiIO_3$ (undoped and doped with Fe) along the hexagonal c-axis in a broad frequency range of 10^{-2} Hz $\leq \nu \leq 10^9$ Hz and at temperatures 100 K $\leq T \leq$ 500 K. Special care has been taken to clarify the influence of space charge accumulation at the electrodes in this material by investigating samples of different thickness. Below approximately 10 kHz, the electric response of the $LiIO_3$ crystals was entirely dominated by blocking electrode effects. At higher frequencies the ac conductivity reveals a power law behaviour, $\sigma \sim \nu^s$, with a relatively low frequency exponent $s < 0.2$ as sometimes found in ionic conductors [32, 33]. The results in the charge dominated region give rise to the assumption of at least two types of ions as charge carriers in α-$LiIO_3$. In addition, the dc measurements provide experimental evidence that electronic conduction plays a role in α-$LiIO_3$ too.

2. Experimental Procedure

α-$LiIO_3$ crystals were obtained by reacting stoichiometric balanced quantities of Li_2CO_3 and HIO_3, followed by slow evaporation at 40 °C of the resultant lithium iodate aqueous solution. The mean crystal growth rate along the c-axis was 0.6 mm/day. The iron doped samples were obtained by adding $FeCl_3$ to the solution, and the final iron doping was 93 ppm (mol). The literature is ambiguous about the position of Fe^{+3} ions in the lithium iodate lattice, but it seems that they substitute both Li^+ and I^{+5} ions, the Li^+ substitution being more probable [34 to 38].

Since there was no HIO_3 excess in the original solution for the iron free samples it is possible to say that the undoped samples were grown in neutral environment, i.e., with pH around 7. On the other side, some HIO_3 had to be added to the solution of the iron doped crystals to prevent iron to precipitate. Anyhow, comparison of the measured frequency response of the dielectric constant at room temperature with that from [13] allows us to confirm our estimate of the pH value. Using the data from [22, 23] it was possible to obtain the hydrogen concentration x of our samples: 0.16 for undoped, and 0.25 for Fe doped.

The conductance and capacitance were measured in broad frequency and temperature ranges employing different experimental set-ups. For the range 0.01 Hz to 10 kHz a frequency response analyser supplemented with a high impedance preamplifer was used (Schlumberger 1260 and Chelsea interface). The frequencies 5 Hz $\leq \nu \leq$ 13 MHz were

studied using the autobalanced bridge HP 4191A. The high frequency range, 1 to 1000 MHz, was covered with an HP 4191A impedance analyzer [39], and the dc measurements were performed using an HP 3457A multimeter. As contacts silver paint or sputtered gold films were applied on both sides of the samples. All measurements have been performed with the electric field directed parallel to the c-axis. Most of the measurements were performed in a nitrogen gas heating system covering the temperature range of 100 to 500 K. In addition, a closed cycle refrigerator and various ovens were used.

3. Results and Discussions

In Fig. 1 and 2 the dielectric constant (upper parts) and the conductivity (lower parts) are shown as a function of frequency for several temperatures and for both, an undoped (Fig. 1) and an iron doped sample (Fig. 2). The results have been obtained using three

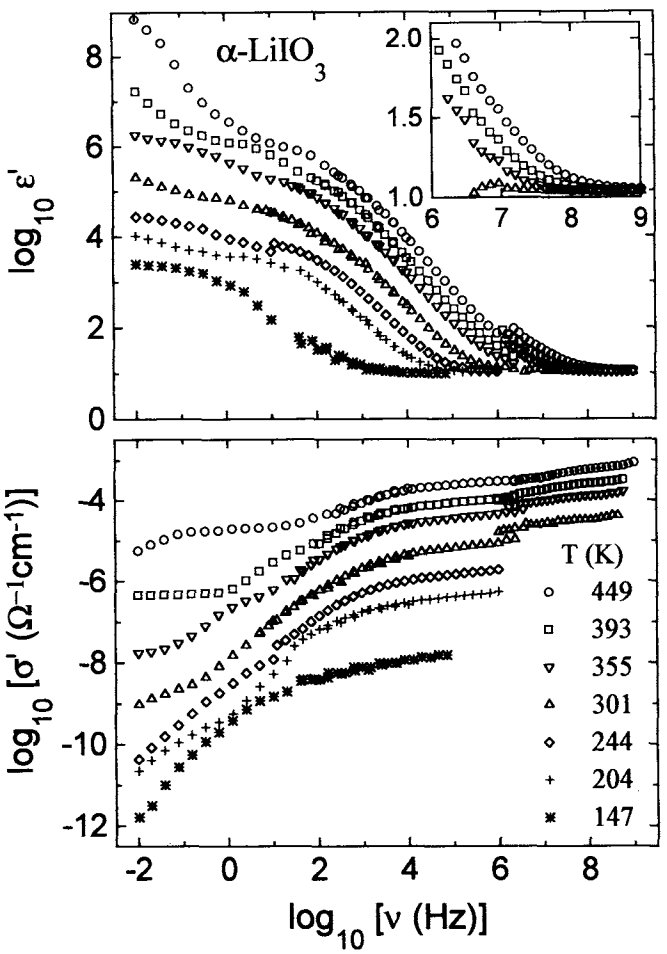

Fig. 1. Frequency dependence of the real parts of the dielectric constant (upper part) and of the conductivity (lower part) of α-$LiIO_3$ for various temperatures (double logarithmic plot). The inset shows a magnified view of the dielectric constant at high frequencies

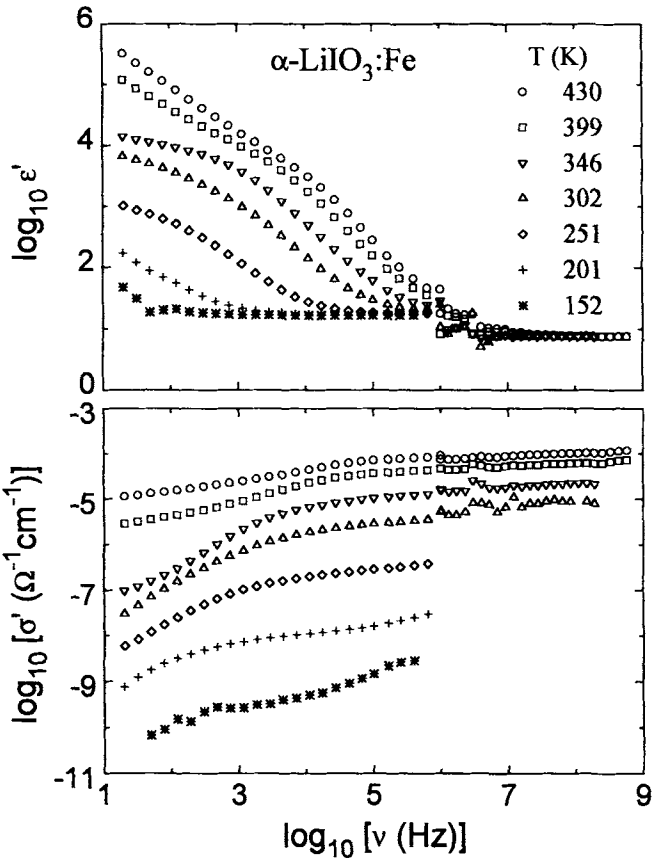

Fig. 2. Frequency dependence of the real parts of the dielectric constant (upper part) and of the conductivity (lower part) of iron doped α-$LiIO_3$ for various temperatures (double logarithmic plot)

(Fig. 1) or two (Fig. 2) different experimental set-ups. The slight offset of the $\varepsilon'(\nu)$ data obtained at high frequencies (1 MHz to 1 GHz) can be attributed to parasitic capacitances inherent to this method. At high frequencies, $\nu > 1$ MHz, and below room temperature, piezoelectric resonances were observed but are not shown in Fig. 1 and 2. The overall behaviour of $\varepsilon'(\nu)$ can be characterized by a large increase with decreasing frequency with a tendency to saturate at low and high frequencies. The point of inflection shifts to higher frequencies as the temperatures increases. After approaching a saturation value for low frequencies, a second increase sets in which is most clearly seen at the highest temperatures investigated. The conductivity $\sigma'(\nu)$ increases with increasing frequency. At high temperatures ($T > 350$ K) the conductivity exhibits a plateau at low frequencies, and at 449 K for the undoped sample a further decrease of $\sigma'(\nu)$ is seen below 0.1 Hz.

To investigate the nature of the results described above we performed measurements for crystals with varying thickness. In this way a significant change of the frequency dependence of ε' and σ' was observed for frequencies $\nu < 10$ kHz. Fig. 3 shows the results obtained at room temperature for two crystals with different geometrical capacitances.

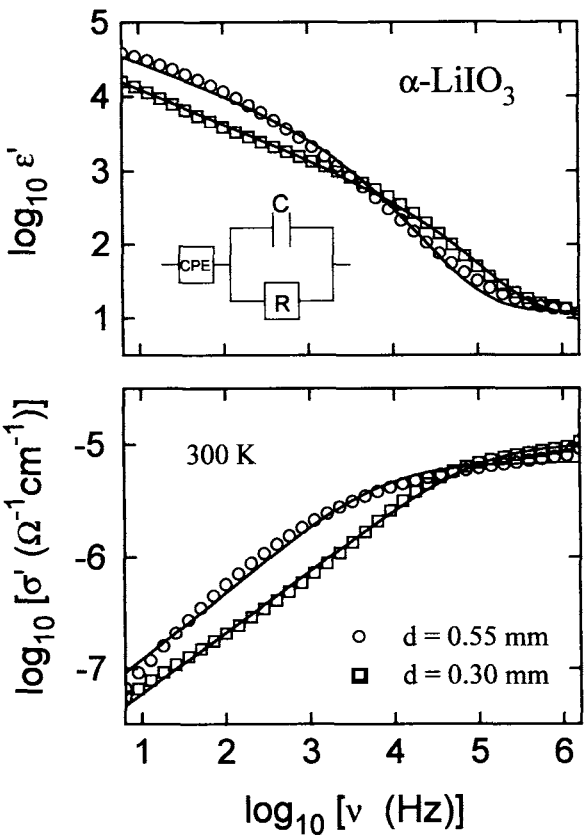

Fig. 3. Frequency dependence of the real parts of the dielectric constant (upper part) and of the conductivity (lower part) at room temperature (double logarithmic plot) as obtained on two samples of α-$LiIO_3$ of different thickness d. The solid lines are the results of least-squares fits using the equivalent circuit indicated in the figure. Here CPE denotes a constant phase element to simulate the blocking electrodes. The sample response is modeled by a lossy capacitor

Clearly, the increase of $\varepsilon'(\nu)$ and the decrease of $\sigma'(\nu)$ shift to higher frequencies when the sample thickness is reduced. This finding is indicative of blocking electrodes which arise from the accumulation of ions near the electrode upon applying an electrical field. Blocking electrodes have already been observed in earlier works on α-$LiIO_3$ [1, 24, 26]. Effects of electrode polarization should occur at the higher frequencies, the thinner the sample is, as indeed is observed in Fig. 3. In addition, as the mobility of the ions increases with temperature, the blocking electrode effects should occur at higher frequencies for higher temperatures, again in accordance with the results of Fig. 1 and 2. The data of Fig. 3 have been fitted using the equivalent circuit indicated in Fig. 3. Here a parallel RC circuit describes the intrinsic sample properties (R and C have been assumed to be frequency independent). For the electrodes a constant phase element (CPE) has been assumed as it is commonly used for the description of blocking electrodes [40]. For the CPE the admittance is given by $Y = A(i\omega)^{\alpha}$. The solid lines are the result of least-squares fits using this equivalent circuit. A reasonably good description of the data has been achieved. Deviations of fit and data are mainly due to the slight frequency dependence of the intrinsic sample properties and the deviations from CPE behaviour at low frequencies. The geometry corrected parameters are: $\varrho_{dc} = 7.7 \times 10^4\ \Omega$ cm, $\varepsilon = 13$, $A = 9.6 \times 10^{-9}\ \Omega^{-1}\ \mathrm{cm}^{-1}\ \mathrm{s}^{0.55}$, $\alpha = 0.55$ for sample thickness $d = 0.30$ mm and $\varrho_{dc} = 1.3 \times 10^5\ \Omega$ cm, $\varepsilon = 13$, $A = 1.8 \times 10^{-8}\ \Omega^{-1}\ \mathrm{cm}^{-1}\ \mathrm{s}^{0.6}$, $\alpha = 0.6$ for $d = 0.55$ mm.

We conclude from these experiments that the electrical response of the α-$LiIO_3$ crystals below 10 kHz is completely determined by electrode effects.

However, the additional increase of $\varepsilon'(\nu)$ and the saturation of $\sigma'(\nu)$ at low frequencies and high temperatures as indicated in Fig. 1 and 2 cannot be explained using the above equivalent circuit. The saturation of $\sigma'(\nu)$ is indicative of an additional conduction contribution which takes over when the main charge carriers which have been shown to be Li^+ ions [9 to 12] are blocked by the electrodes. From an Arrhenius plot of the saturation value of σ' we obtained an energy barrier of 0.99 eV. The additional increase of $\varepsilon'(\nu)$ and the onset of a decrease of $\sigma'(\nu)$ seen for the undoped sample at 449 K can only be explained assuming a second blocking of the electrodes due to a different kind of ions with a lower mobility than that of the Li^+ ions. In this context it is interesting that there are reports of hydrogen ions contributing to the conductivity in $LiIO_3$ [12, 41, 42].

From the above discussion it is clear that only at frequencies above 10 kHz the bulk electric properties of α-$LiIO_3$ are measured. In this range the dielectric constant approaches its high frequency limit ε_∞ (Fig. 1 and 2). The temperature dependence of ε_∞ is shown in Fig. 4. For both samples ε_∞ is only weakly temperature dependent. In the double logarithmic representations of Fig. 1 and 2 the conductivity at high frequencies exhibits a slow increase with constant slope, i.e., it can be described by a power law $\sigma' \sim \nu^s$ with $s \approx 0.16$ for undoped α-$LiIO_3$ and $s \approx 0.06$ for α-$LiIO_3$:Fe. Such a behaviour has been termed low frequency dispersion (LFD) and is often observed in ionic conductors at low frequencies [32, 43, 44]. Usually at high frequencies there is a transition from LFD to a power law with a considerably higher slope, $s > 0.5$ [32], which can be attributed to conduction by hopping processes [32, 45, 46]. However, this hopping region obviously does not occur in α-$LiIO_3$ in the frequency range investigated (Fig. 1) and in α-$LiIO_3$:Fe only at temperatures below around 200 K (Fig. 2), leaving LFD as dominant process up to frequencies of 1 GHz. Jonscher [32, 44] proposed electrochemical

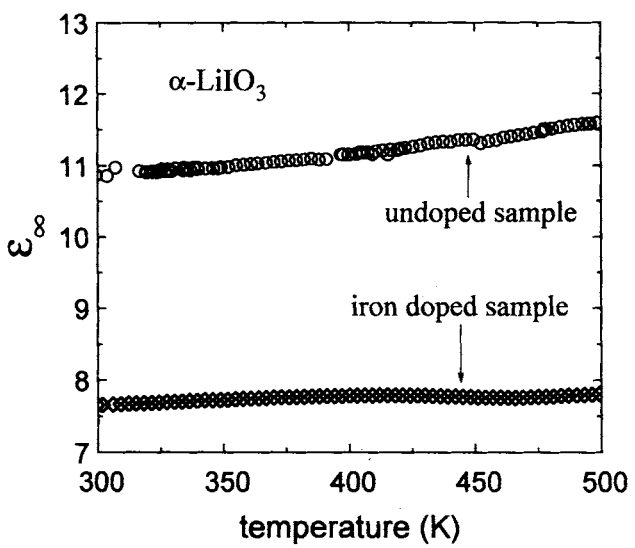

Fig. 4. Temperature dependence of the high frequency limit of the dielectric constant for undoped and iron doped α-$LiIO_3$

processes as origin of the LFD behavior but up to now there is no commonly accepted theoretical explanation for LFD. In the frequency dependence of the dielectric constant the LFD should show up as power law, $\varepsilon' \sim \nu^{s-1}$ [32]. However, in our measurements the detection of this power law is hampered by the dominating ε_∞ and by blocking electrode effects.

To investigate the temperature dependence in the region of the intrinsic sample response we plotted $\sigma' T$ versus the inverse temperature at 100 kHz (Fig. 5). This plot should give a straight line for the dc conductivity of an ionic conductor according to the simple model of Lidiard [47]. For temperatures $T > 280$ K straight lines are observed for both samples. The activation energies obtained from the slopes are: 0.32 eV for the undoped sample and 0.30 eV for the iron doped sample. At lower temperatures the slope changes significantly with activation energies of 0.17 and 0.14 eV for $LiIO_3$ and $LiIO_3$:Fe, respectively, which are approximately half the values at higher temperatures. Such a behaviour is often observed in ionic conductors and can be understood assuming that at high temperatures the conductivity is determined both by the activation energy for the motion of an ion from one potential well to another and by the activation energy for the formation of a "free" ion [47]. At low temperatures only the activation of motion dominates the temperature dependence of σ'. The deviations from linear behaviour seen in Fig. 5 at the lowest temperatures may well be due to the onset of hopping conductivity. We want to mention that a similar behaviour as shown in Fig. 5 has been reported by Abramovich et al. [29] for crystals grown from a solution with a pH value of 2.

Now, we want to give an alternative representation of the ac data presented above using the modulus formalism [48, 49]. The electric modulus M is defined as the inverse of the complex dielectric constant. It is well known that the representation of the dielectric data as $M(\nu)$ suppresses the effects of blocking electrodes which makes it especially well suited for the data presented in this work. However, we have a mention that there is a large controversy about the use of this representation and the interpretation of dielectric data connected to it [49, 50]. Fig. 6 shows the frequency dependence of the ima-

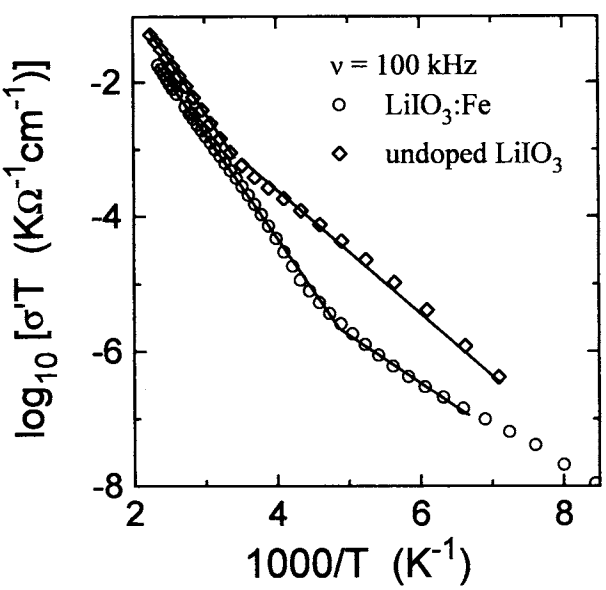

Fig. 5. Arrhenius plot of the real part of the conductivity multiplied by the temperature for undoped and iron doped α-$LiIO_3$ at 100 kHz. The solid lines indicate thermally activated behaviour

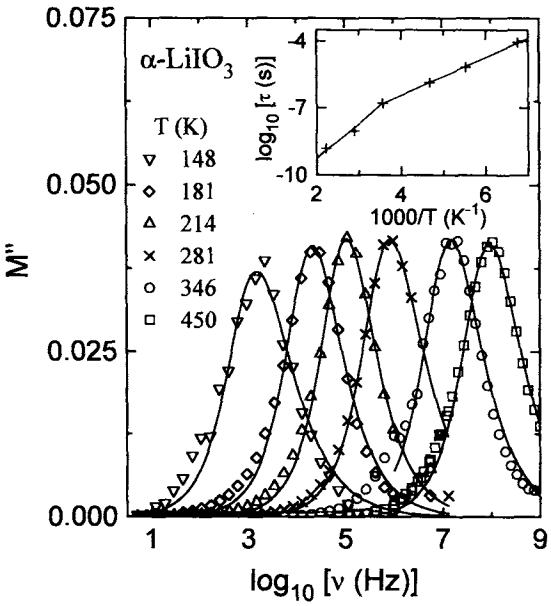

Fig. 6. Frequency dependence of the imaginary part of the dielectric modulus of α-$LiIO_3$ at various temperatures. The lines are the results of least-squares fits using the Fourier transform of the KWW function. The inset shows the temperature dependence of the KWW relaxation time in an Arrhenius representation. The lines correspond to thermally activated behaviour

ginary part of the modulus of α-$LiIO_3$ for various temperatures. As observed in many ionic conductors, a peak shows up which shifts to higher frequencies with increasing temperature. It can be interpreted as indication of a so-called conductivity relaxation [48, 49]. The peak can be fitted using the Fourier transform of the Kohlrausch-Williams-Watts (KWW) function, $\varphi(t) = \varphi_0 \exp(-t/\tau)^{\beta}$, where β is the stretching exponent determining the width and asymmetry of the peak. The blocking electrode effects show up as slight deviations from KWW behaviour at low frequencies. The resulting β is almost temperature independent with a value of approximately 0.8 which indicates a distribution of conductivity relaxation times. Usually in ionic conductors the energy barrier obtained from the modulus evaluation is identical to that of the dc conductivity taken from the saturation value of the conductivity at frequencies above the blocking electrode regime. The inset of Fig. 6 shows the relaxation time τ in an Arrhenius representation. $\tau(T)$ can well be described assuming two thermally activated processes with energy barriers 0.16 and 0.30 eV which are almost identical to the energy barriers obtained from $\sigma(T)$ (Fig. 5), as expected. There are no signs of a relaxation process in the kHz region as sometimes reported [25, 29, 30]. However, one has to aware that blocking electrode effects are easily mistaken for (intrinsic) relaxational behaviour.

In addition, we measured the dc conductivity of α-$LiIO_3$ with completely blocked electrodes to detect possible electronic contributions to the conductivity. For this purpose, prior to the measurement, the dc field was applied for 60 h. At 450 K the conductivity is about $10^{-9}\ \Omega^{-1}\ \mathrm{cm}^{-1}$ and its temperature dependence follows a thermally activated behaviour with an energy barrier of 0.74 eV. Since this value is much lower than the reported electronic gap energy of about 4.3 eV, determined from optical measurements [3], the charge carriers most probably are electrons or holes from defect states in the gap.

Finally, we have not observed any sign of the anomaly around 243 K mentioned in [30] and [51]. The authors suggest that hydrogen may play an important role in this phenomenon since it was observed in acid crystals only.

4. Conclusions

We have performed a detailed investigation of the dc and ac electrical properties of α-$LiIO_3$ (undoped and doped with Fe) in a broad frequency range. At frequencies below approximately 10 kHz the electrical properties of the samples were almost completely dominated by space charge effects at the electrodes. The results in this frequency region give evidence for at least two types of ionic charge carriers in α-$LiIO_3$, most probably Li^+ and H^+. At higher frequencies the ac conductivity reveals a power law behaviour, $\sigma' \sim \nu^s$, with a small exponent $s \approx 0.16$ for undoped α-$LiIO_3$ and $s \approx 0.06$ for the iron doped compound. This behaviour resembles the so-called low frequency dispersion often found in ionic conductors [32, 43, 44]. The dielectric constant approaches its high frequency limit $\varepsilon_\infty \approx 11.3$ for α-$LiIO_3$ and $\varepsilon \approx 7.7$ for α-$LiIO_3$:Fe which is only weakly temperature dependent for both compounds. The temperature dependence of the conductivity in the high frequency region behaves thermally activated with an energy barrier of approximately 0.3 eV for both compounds. Below temperatures around 250 K, a significant reduction of the energy barrier is observed which can be understood by a simple model for ionic conductivity [47]. The modulus representation of the obtained dielectric data leads to well developed peaks in $M''(\nu)$ which can be interpreted as being due to the occurrence of conductivity relaxation [48, 49]. Fits of $M''(\nu)$ using the Fourier transform of the KWW function reveal a stretching exponent $\beta \approx 0.8$ which indicates a distribution of conductivity relaxation times. The energy barriers connected to the conductivity relaxation are almost identical to those obtained from the conductivity in the LFD regime. The results of the dc investigations give clear indications that electronic conductivity involving defect states plays an important role, too.

Acknowledgement This research was supported by Volkswagen-Stiftung under the contract number I-64764.

References

[1] S. Haussühl, phys. stat. sol. **29**, K159 (1968).
[2] A. W. Warner and D. A. Pinnow, J. Acoust. Soc. Amer. **47**, 791 (1970).
[3] F. R. Nash. J. G. Bergman, G. D. Boyd, and E. H. Turner, J. appl. Phys. **40**, 5201 (1969).
[4] S. K. Kurtz, T. T. Perry, and J. G. Bergman, Jr., Appl. Phys. Letters **12**, 186 (1968).
[5] W. H. Zachariasen and F. A. Barta, Phys. Rev. **37**, 1626 (1931).
[6] H. Arend, M. Remoissenet, and W, Staehlin, Mater. Res. Bull. **7**, 869 (1972).
[7] C. Galez, C. Rosso, Y. Teisseyre, J. M. Crettez, P. Bourson, G. Medeiros- Ribeiro, A. Righi, and R. L. Moreira, Solid. State Commun. **93**, 1013 (1995).
[8] A. A. Blistanov, V. V. Geraskin, N. S. Kozlova, E. V. Makarevskaya, and O. G. Portonov, Soviet Phys. – Cryst. **32**, 703 (1987).
[9] Y. Y. Li, Ferroelectrics **35**, 167 (1981).
[10] O. G. Vlokh, I. A. Velichko, and L. A. Lazko, Soviet Phys. – Cryst. **20**, 263 (1975).
[11] L. Jiarui and Z. Qichu, Solid State Commun. **63**, 307 (1987).
[12] R. Lutze, W. Gieseke, and W. Schröter, Solid State Commun. **23**, 215 (1977).
[13] M. Remoissenet and J. Garandet, Mater. Res. Bull. **10**, 181 (1975).
[14] V. I. Bredikhin, L. A. Dmitrenko, N. V. Korolikhin, M. A. Kotova, M. A. Novikov, and V. I. Rubakha, Soviet Phys. – Cryst. **27**, 557 (1982).
[15] A. Yu. Klimova, A. F. Konstantinova, Z. B. Perekalina, N. A. Baturin, and G. F. Dobrzhanskii, Soviet Phys. – Cryst. **28**, 699 (1983).
[16] A. Yu. Klimova, K. I. Avdienko, and B. I. Kidyarov, Soviet Phys. – Cryst. **34**, 279 (1989).

[17] J. M. DESVIGNES and M. REMOISSENET, Mater. Res. Bull. **6**, 705 (1971).
[18] L. S. GOLDBERG, Appl. Optics **14**, 653 (1975).
[19] V. V. VOROBEV, A. A. KULESHOV, E. V. CHARNAYA, A. A. ABRAMOVICH, S. V. ALCHANGYAN, B. I. KIDYAROV, and M. N. KULBITSKAYA, Soviet Phys. – Solid State **31**, 1670 (1989).
[20] V. V. VOROBEV, E. P. LOKSHIN, and E. V. CHARNAYA, Soviet Phys. – Solid State **34**, 478 (1992).
[21] N. A. BATURIN, A. F. KONSTANTINOVA, Z. B. PEREKALINA, G. F. DOBRZHANSKII, and V. M. ZATONSKAYA, Soviet Phys. – Cryst. **30**, 474 (1985).
[22] S. A. HAMID, G. KUNZE, and G. REUTER, Acta cryst. **A33**, 261 (1977).
[23] S. A. HAMID and G. KUNZE, Acta cryst. **A33**, 264 (1977).
[24] H. THOMANN, Z. angew. Phys. **32**, 311 (1972).
[25] G. ARLT, W. PUSCHERT, and P. QUADFLIEG, phys. stat. sol. (a) **3**, K243 (1970).
[26] E. SAILER, phys. stat. sol. (a) **4**, K173 (1971).
[27] B. V. SHCHEPETILNIKOV, A. I. BARANOV, and L. A. Shuvalov, Soviet Phys. – Solid State **29**, 450 (1987).
[28] A. A. ABRAMOVICH, V. A. SHUTILOV, T. D. LEVITSKAYA, B. I. KIDYAROV, and P. L. MITNITSKII, Soviet Phys. – Solid State **14**, 2237 (1973).
[29] A. A. ABRAMOVICH, A. SH. AKRAMOV, A. É. ALIEV, and L. N. FERSHTAT, Soviet Phys. – Solid State **29**, 1426 (1987).
[30] A. E. ALIEV, A. SH. AKRAMOV, L. N. FERSHTAT, and P. K. KHABIBULLAEV, phys. stat. sol. (a) **108**, 189 (1988).
[31] A. E. ALIEV, A. SH. AKRAMOV, and R. R. VALETOV, Soviet Phys. – Solid State **31**, 2127 (1989).
[32] A. K. JONSCHER, Dielectric Relaxation in Solids, Chelsea Dielectrics Press, Ltd., London 1983.
[33] A. K. JONSCHER, Nature (London) **267**, 673 (1977).
[34] W. KARTHE, Acta phys. Polon. S **47**, 553 (1975).
[35] L. M. BELYAEV, B. N. GRECHUSHNIKOV, G. F. DOBRZHANSKII, N. N. DYMENKO, YU. N. MARTYSHEV, Z. B. PEREKALINA, and M. S. SMORODINA, Soviet Phys. – Cryst. **22**, 372 (1977).
[36] V. O. MARTIROSYAN, M. L. MEILMAN, I. N. MAROV, V. V. ZHUKOV, and K. T. SEVINYAN, phys. stat. sol. (b) **72**, 441 (1975).
[37] V. O. MARTIROSYAN, M. L. MEILMAN, R. O. SHARKHATUNYAN, B. N. GRECHUSHNIKOV, and V. F. KORYAGIN, Soviet Phys. – Solid State **16**, 2025 (1975).
[38] A. BRÄUER and D. M. DARASELIYA, Soviet Phys. – Solid State **19**, 1318 (1977).
[39] R. BÖHMER, M. MAGLIONE, P. LUNKENHEIMER, and A. LOIDL, J. appl. Phys. **65**, 901 (1989).
[40] J. R. MCDONALD (ED.). Impedance Spectroscopy, John Wiley & Sons, New York, 1987.
[41] H. NÄGERL and S. HAUSSÜHL, phys. stat. sol. (a) **3**, K203 (1970).
[42] V. V. VOROBEV and E. V. CHARNAYA, Soviet. Phys. – Solid State **33**, 820 (1991).
[43] A. K. JONSCHER, Phil. Mag. **B38**, 587 (1978).
[44] A. K. JONSCHER, J. Mater. Sci. **26**, 1618 (1991).
[45] S. R. ELLIOTT, Adv. Phys. **36**, 135 (1987).
[46] A. R. LONG, Adv. Phys. **31**, 553 (1982).
[47] S. FLÜGGE (Ed.), Encyclopedia of Physics, Vol. XX, Springer-Verlag, Berlin 1957 (p. 246ss).
[48] P. B. MACEDO, C. T. MOYNIHAN, and R. BOSE, Phys. Chem. Glasses **13**, 171 (1972).
[49] C. T. MOYNIHAN, J. non-crystall. Solids **172/174**, 1395 (1994).
[50] S. R. ELLIOTT, J. non-crystall. Solids **170**, 97 (1994).
[51] J. DEL CERRO, S. RAMOS, and J. ISIDORO, phys. stat. sol. (a) **72**, K23 (1982).